Potassium Selective Calix[4]semitubes

Philip R. A. Webber,[a] Andrew Cowley,[a] Michael G. B. Drew,[b] and Paul D. Beer*[a]

Abstract: A new class of ionophore consisting of two calix[4]arene units linked through the lower rim by two ethylene chains, in combination with propyl ether and phenolic functional groups, has been developed. These calix[4]semitube molecules exhibit remarkable selectivity and fast complexation kinetics for potassium over all Group 1 metal cations. Molecular modelling studies, using structural models derived from crystallographic data, suggest the potassium cation is complexed by a horizontal, side-on route and not through the calix[4]arene annulus. The length of the bridging alkylene chain between the respective calix[4]arenes of the semitube structure dictates the strength and selectivity of alkali metal cation binding.

Keywords: alkali metals · calixarenes · ionophores · potassium · supramolecular chemistry

Introduction

The design and synthesis of new ionophores for alkali metals is a continuing area of intense research activity.[1] In particular, the recent structural determination of the *Streptomyces lividans* potassium channel[2] has stimulated further research into elucidating the essential structural and mechanistic features of ion channels through the construction of abiotic systems.[3] The calixarene structural framework has been modified to produce a series of potassium selective ligands.[4] Notable examples include the tetraacetates of 1,3-alternate calix[4]arene[5] and dioxacalix[4]arene,[6] the hexaacetate of calix[6]arene[7] and a 1,3-alternate calix[4]crown receptor, which displays higher K^+/Na^+ selectivity than the natural ionophore valinomycin.[8] The cation specificity of these molecules can be attributed to the presence of multiple hard oxygen donor atoms, a complementary cation-to-cavity size, the degree of host preorganisation and, for the last receptor at least, aromatic π–cation interactions.

We have recently reported a new class of cryptand-type ionophore, the calix[4]tube **I**,[9] based on a bis(calix[4]arene) scaffold that displays exceptional selectivity for potassium over all other Group 1 metal cations and barium. The slow kinetics of potassium cation uptake by calix[4]tubes has lead us to design less rigid ionophores, the calix[4]semitubes **II** that consist of two calix[4]arene moieties connected by two bridging alkylene chains. In this paper we report the synthesis, coordination chemistry and modelling investigations of these novel ionophores that exhibit fast complexation kinetics whilst retaining remarkable potassium cation selectivity.

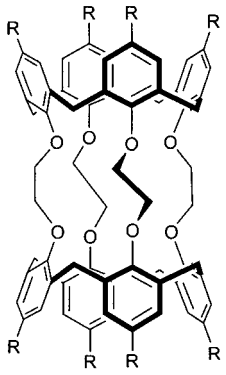

Ia R = *t*Bu

Ib R = *t*Oct

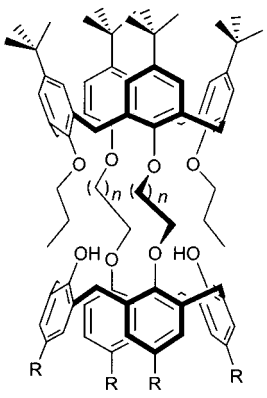

II

n = 1, 3; R = *t*Bu, H

Results and Discussion

Synthesis: Taking into account the calix[4]tube structure[9] in which the calix[4]arene units impart a size discriminatory filter for the entry of metal cations through the calix[4]arene annulus, our new receptor design features two calix[4]arene moieties linked by two alkylene groups only, with propyl ether

[a] Prof. P. D. Beer, Dr P. R. A. Webber, Dr A. Cowley
Department of Chemistry
Inorganic Chemistry Laboratory
University of Oxford
South Parks Road, Oxford OX1 3QR (UK)
Fax: (+44) 1865-272-690
E-mail: paul.beer@chem.ox.ac.uk

[b] Prof. M. G. B. Drew
Department of Chemistry
University of Reading
Whiteknights, Reading RG6 2AD (UK)

 DOI: 10.1002/chem.200204518

and phenolic −OH functional groups making up the eight oxygen-donor recognition site for alkali metal complexation.

The target calix[4]semitubes were prepared according to the synthetic route shown in Scheme 1. The reaction of 1,3-dipropoxy lower-rim substituted calix[4]arene **1** with two equivalents of the appropriate bromoalkyl ethyl ester in the presence of sodium hydride gave the ester–ether products **2** and **3** in yields of 85% and 46%, respectively.[10] Lithium aluminium hydride reduction in tetrahydrofuran gave the corresponding alcohols **4** and **5**, which on reaction with tosyl chloride, gave the tosylates **6** and **7** in good overall yields. Refluxing a mixture of the appropriate calix[4]arene and calix[4]arene tosylate in acetonitrile in the presence of excess potassium carbonate for seven to ten days gave the new calix[4]semitubes **8**, **9** and **10** in yields of 53%, 56% and 71%, respectively. All calix[4]semitubes were characterised by ^{1}H and ^{13}C NMR spectroscopy, mass spectrometry and elemental analysis (see Experimental Section).

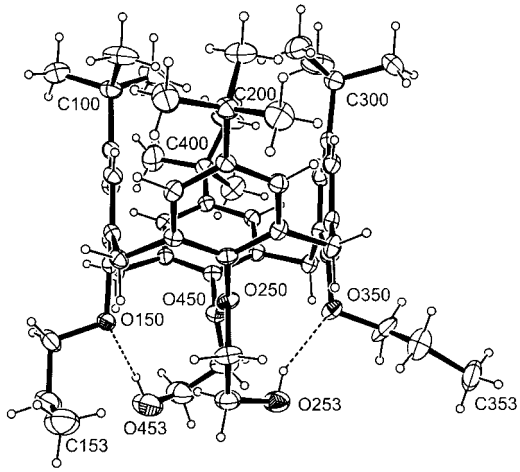

Figure 1. The structure of **4** with ellipsoids at 20% probability. Hydrogen bonds are shown as dotted lines.

X-ray crystal structures of 4 and calix[4]semitube 9: Single crystals of **4** were grown by slow evaporation from a dilute solution of the compound in dichloromethane/methanol. The structure of **4** is shown in Figure 1. The calix[4]arene adopts the well-known distorted cone conformation with approximate C_2 symmetry, in which two of the phenyl rings are roughly parallel to the cone axis with angles of intersection with the plane of the four methylene groups of 86.6 and 86.2°. The other two rings are semihorizontal making angles of 43.2 and 46.7° with this plane. There is no solvent in the unit cell, nor are there any intermolecular hydrogen bonds. Instead the two −OH groups O253 and O453 form hydrogen bonds to the other oxygens O150 and O350 at distances of 2.99 and 2.74 Å, respectively.

Crystals of **9**, suitable for X-ray diffraction, were grown by slow evaporation from a solution of the ligand in chloroform/methanol. The structure of **9** (Figure 2) reveals that both calix[4]arene moieties in the molecule take up cone conformations. The unsubstituted calix[4]arene has a regular cone structure in which the four phenyl rings intersect the plane of the four methylene carbon atoms at consecutive angles of 41.6, 68.4, 55.6 and 62.3°. However, the tetra-*tert*-

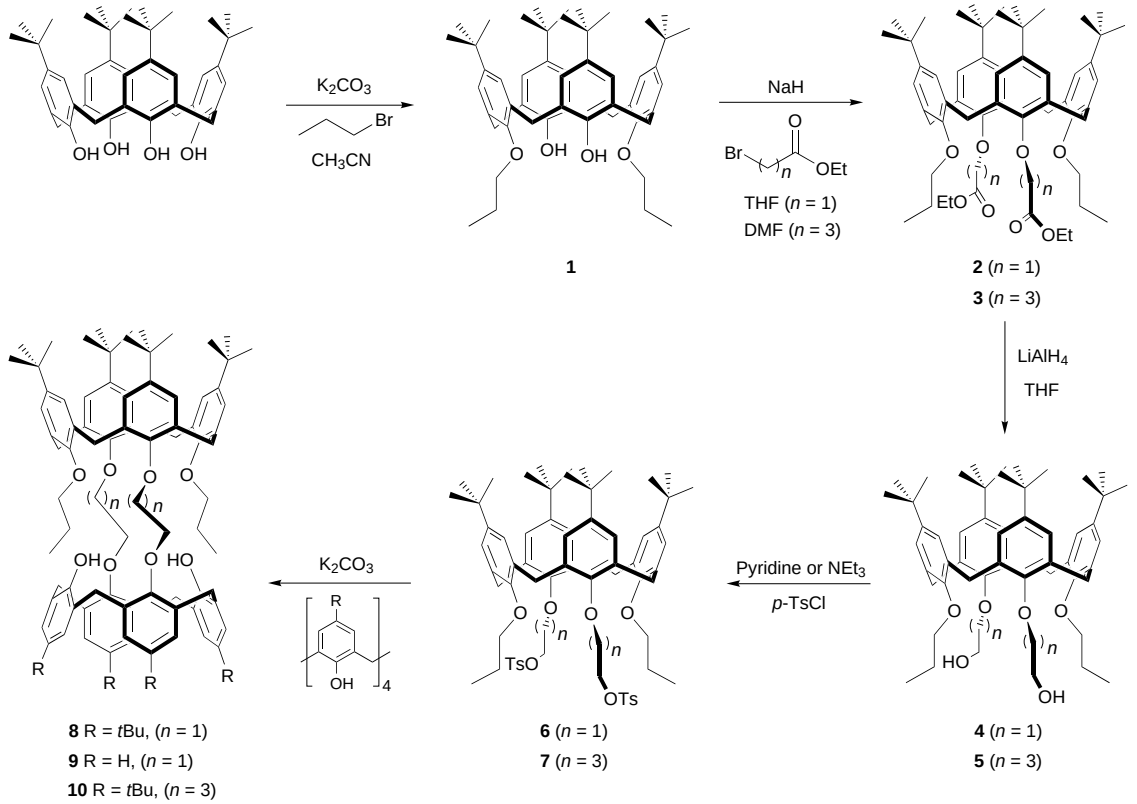

Scheme 1. Synthesis of the calix[4]semitubes. Ts = toluene-4-sulphonyl.

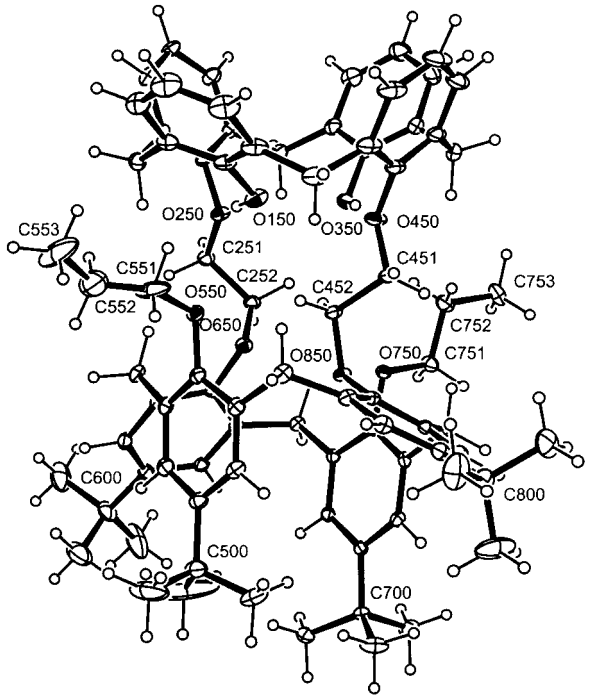

Figure 2. The structure of **9** in crystals of **9**·$CHCl_3$. Ellipsoids are drawn at 20% probability. The chloroform molecule is not shown.

butylcalix[4]arene has the more distorted cone conformation with the four phenyl rings intersecting the plane of the four methylene carbon atoms at consecutive angles of 75.6, 46.1, 83.2 and 24.9°. The ether linkages between the two calix[4]-arenes have different conformations as measured by the torsion angles of the five bonds, which starting from the *tert*-butyl end are 116.0, 145.0, 163.4, 43.8, 67.8 and −71.8, 148.1, 86.6, 89.6, −60.8°. Thus, the two central O-C-C-O torsion angles are *trans* (163.4°) and *gauche* (86.6°).

Coordination studies

^{1}H NMR complexation investigations: Preliminary experiments were undertaken on calix[4]semitubes **8** and **9** to establish their kinetic complexation behaviour towards Na^+, K^+ and Rb^+ ions. The addition of one equivalent of $NaClO_4$, KSCN or $RbPF_6$ to solutions of the respective calix[4]semitubes in 1:1 $CDCl_3/CD_3OD$ revealed that although the complexation/decomplexation process was slow on the NMR timescale, the time required for each complexation to reach equilibrium was fast, at least shorter than the time taken to procure the NMR titration experiment, which was less than 4 minutes. This contrasts with calix[4]tube **I** for which a heterogeneous mixture of 20 equivalents of KI and **I** in 4:1 $CDCl_3$:CD_3OD took just under 2 h to reach equilibrium.[9]

Stability constants for **8** and **9** with alkali metal cations were determined by direct integration of host and complex resonances in the ^{1}H NMR spectrum; these values are shown in Table 1. As was hoped, both calix[4]semitubes display excellent K^+ selectivity. In fact, both ligands are 100% complexed upon addition of one equivalent of K^+. The solubility properties of **8** and **9** precluded complexation studies being carried out in more competitive solvent mixtures. In comparison, the information from Table 1 shows that **8** and **9** form very weak complexes with Na^+ and Rb^+ and that no evidence of complexation was observed with Cs^+.

Table 1. Stability constant data for the alkali metal complexes.

	K [M^{-1}][a]	
	8	**9**
Na^+	20	5
K^+	$>10^5$	$>10^5$
Rb^+	30	20
Cs^+	0	0

[a] Determined in 1:1 $CDCl_3$:CD_3OD at 291 K. The alkali metal cations were added as their perchlorate, thiocyanate or hexafluorophosphate salts.

Figure 3 reveals how the ^{1}H NMR spectrum of **9** changes with increasing equivalent amounts of K^+. The two singlets at around 6.15 and 6.8 ppm in free **9**, due to the ArH protons on the calixarene bearing the propyl groups, give strong evidence that this calixarene in the receptor adopts the C_2-distorted cone conformation in solution. The chemical shift values of the remaining ArH protons indicate that the other calixarene in the molecule adopts a regular cone conformation. Both of these facts demonstrate that the structure seen in solution is similar to that in the solid state. Upon complexation, large structural alterations are apparent from the significant changes seen in the ^{1}H NMR spectrum. Most notably, the positioning of the ArH resonances would tend to suggest that both calixarene moieties in the complex adopt regular cone conformations. Interestingly, the propyl $-CH_3$ protons shift upfield by about 0.6 ppm to −0.4 ppm upon complexation. This is surprising because in the crystal structure of free **9**, this CH_3 group is quite distant from any potential source of interaction. For such a large upfield shift to occur, these CH_3 groups probably move inwards and reside over the faces of the free phenolic units of the adjacent calixarene moiety.

Analogous ^{1}H NMR studies of Group 1 metal-cation coordination with the butyl-linked calix[4]semitube **10** containing a larger cavity revealed no evidence of complexation of any of the alkali metal cations in 1:1 $CDCl_3/CD_3OD$. This observation suggests that the length of the bridging alkylene chain between the respective calix[4]arenes of the calix[4]semitube structure critically determines the strength of complexation and Group 1 selectivity preferences for this new class of ionophore.

Molecular modelling: Molecular modelling was undertaken in an effort to ascertain the mode of entry of potassium into the calix[4]semitube, and account for this ionophore's remarkable selectivity and fast kinetics of potassium cation binding.

In the X-ray crystal structure of **9**, it is seen that the two ether spacers have different conformations, one being *trans* and the other *gauche*. These differences are rather surprising as in the calix[4]tube such linkages are equivalent. The calix[4]tube has four linkages that lead to increased rigidity. Perhaps, therefore, it is not surprising that the linkages on opposite sides of the central cavity were always equivalent so that in the absence of metal ions the four linkages were alternately *gauche* and *trans* (*gtgt*), while with an encapsulated metal, the four linkages were all necessarily *gauche* (*gggg*), so that the metal could bond to all eight oxygen atoms.

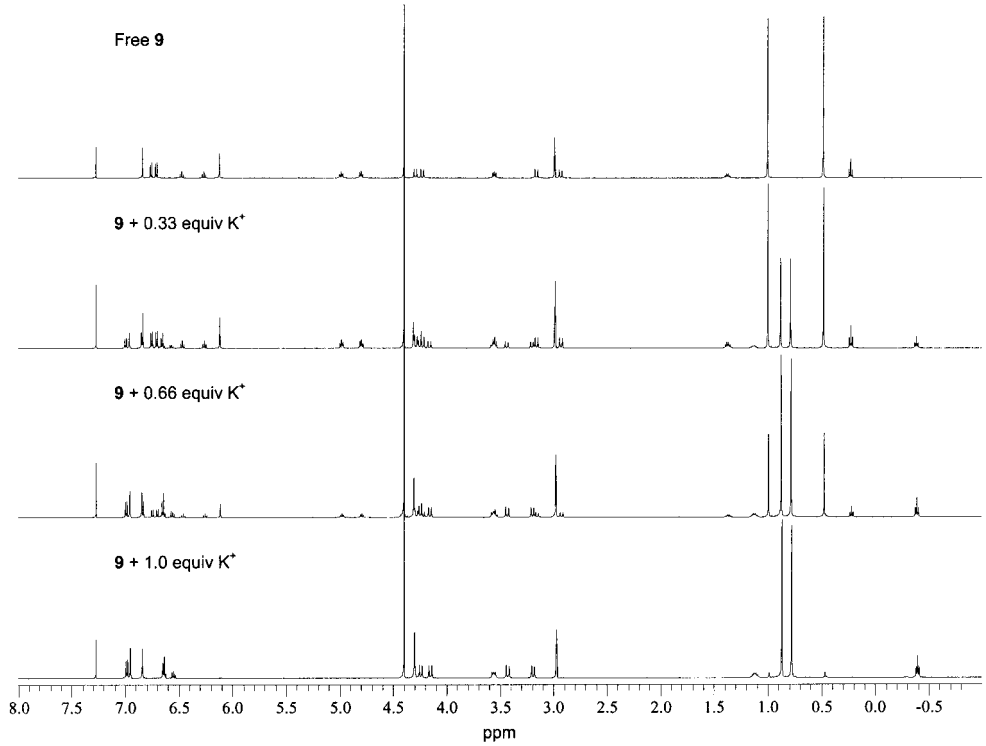

Figure 3. Changes in the ^{1}H NMR spectrum of **9** in the presence of specified equivalents of K^+ (500 MHz, 1:1 $CDCl_3$:CD_3OD).

The established mechanism[9], [11–12] for the insertion of metal ions into calix[4]tubes is illustrated by the crystal structures of **Ia**, **Ib**·Tl_2^{2+} and **Ia**·K^+ shown in Figure 4a–c. This series represents the three stages in the introduction of metals ions into the cavity. Initially, the calix[4]tube is uncomplexed (Figure 4a). In the second stage, the metal enters the top of the calixarene and forms an intermediate complex interacting with the aromatic rings (Figure 4b). The metal then proceeds into the centre of the calix[4]tube and forms bonds to the eight oxygen atoms (Figure 4c).

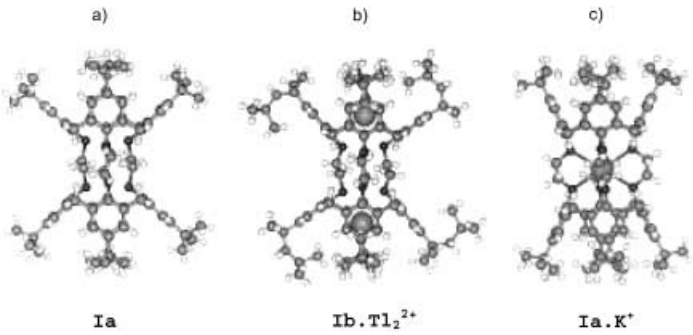

Figure 4. The three stages of metal encapsulation within calix[4]tubes illustrated by the crystal structures of **Ia**, **Ib**·Tl_2^{2+} and **Ia**·K^+.

In **Ia**, both parts of the calix[4]tube have the C_2-distorted cone conformation with links that can be described as *tgtg* (signs ignored), with alternate O-C-C-O torsion angles *trans* and *gauche*. In **Ib**·Tl_2^{2+}, metal ions have entered the calix[4]tube and, while the conformation remains the same, the metals ions now interact with the phenyl rings at each end in an intermediate position. In **Ia**·K^+, the metal ion has now reached the centre of the calix[4]tube. This is accompanied by a change in conformation of the cage so that all four torsion angles are now *gauche* enabling all eight oxygen atoms to bond to the metal ion. The conformations of the individual calix[4]arenes in the calix[4]tube both change from C_2-distorted cones to regular cones.

In previous molecular dynamics simulations[12, 13, 19] we modelled the formation of metal complexes of the *tert*-butyl-calix[4]tube. We now report a study of K^+ within **9** to explain its remarkable selectivity for potassium and its fast kinetics of complexation relative to that observed in the calix[4]tube.

We first calculated the hole size of the macrocycle by inserting K^+ into the centre of the macrocycle in the *gg* cone/cone conformation, fixing the K–O distances at specific values (from 2.3 to 3.3 Å at 0.5 Å intervals) and allowing the macrocycle to relax its conformation by means of molecular mechanics. A resulting plot of energy against K–O distance provided a minimum at 2.84 Å, exactly the same value as was obtained previously for the calix[4]tube and ideally suited for the complexation of K^+.

A conformation analysis on **9** by using molecular dynamics was then performed. The simulation was carried out at 3000 K with a stepsize of 1 fs. A total of 1000 conformations were saved at 1 ps intervals and subsequently optimised with molecular mechanics with the Cerius2 software. All low energy structures showed both O-C-C-O linkages to be *trans* and were therefore different from that observed in the crystal structure of **9** which was located in the analysis but with an energy higher by about 25 kcal mol^{-1}. However, the cone–cone conformation was maintained in all 1000 energy con-

formations; therefore, it seemed appropriate to use the cone–cone conformation with the *tt* conformation in further calculations.

We next investigated the likely mode of entry of potassium ions into the macrocycle. For **9**, there are three possible modes of entry down the axis as shown in Figure 5; from either a) the tetra-*tert*-butyl end or b) the unsubstituted end or c) through a horizontal route perpendicular to the main axis. In the calix[4]tube the horizontal route was shown to be highly unlikely but it was far more accessible for **9** as there were only two linkages between the calix[4]arenes; this led to a more open cage.

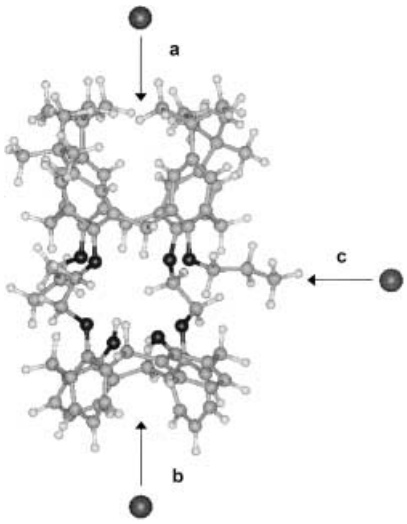

Figure 5. Three possible modes of entry of a cation into the cavity of **9**: a) vertically from the *tert*-butyl end, b) vertically from the unsubstituted end and c) horizontally.

Accordingly, we carried out molecular mechanics calculations to investigate the three possible pathways. The metal ion was positioned at the centre of the macrocycle and moved at 0.5 Å intervals in the three possible directions a, b and c. At each position the macrocycle was allowed to relax around the metal and the energy of the metal complex was calculated. The resulting energies are plotted in Figure 6.

The shape of the curve for path b, the vertical route from the unsubstituted end, is similar in shape to that observed for the calix[4]tube and shows an energy minimum around 4.5 Å for the intermediate position whereby the metal associates with the phenyl rings, although the energy maximum at around 2 Å is not so significant as in the case of the calix[4]tube. However, a minimum energy for an intermediate position is not observed in either curves a or c showing that the metal can follow a low energy path into the metal cavity. These calculations show that all three entry paths were possible.

The mode of insertion of K^+ into the macrocycle was also investigated by molecular dynamics. We carried out three sets of simulations to establish by which path the metal was likely to enter the macrocycle. In each starting model, the metal ion was positioned at about 8 Å from the centre of the cavity along each path as shown in Figure 5. The simulations were

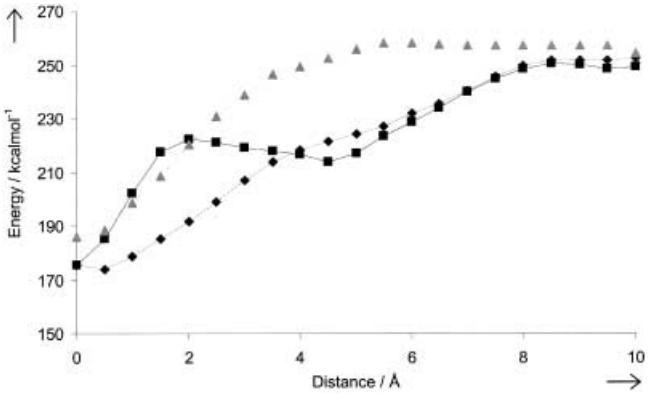

Figure 6. The molecular mechanics energy obtained by moving the metal ion along the entry path into the macrocycle **9**. The distance plotted is that from the centre of the macrocycle. a) diamonds by the vertical route from the *tert*-butyl end, b) squares by the vertical route from the unsubstituted end and c) triangles by the horizontal route.

carried out at a variety of temperatures with no constraints to test the likelihood of each path being followed. The horizontal route was successfully followed by the metal ion at 350 K, a temperature significantly lower than that which proved possible for the completion of the other routes. Snapshots of this simulation are shown in Figure 7. The metal ion moved around its starting position for the first 210 ps with the macrocycle remaining in its original conformation (Figure 7a). After 215.6 ps the metal began to move towards the cavity (Figure 7b) and it had nearly reached the cavity by 216.3 ps (Figure 7c). By 216.67 ps it had completed its move (Figure 7d) and was interacting with all eight oxygen atoms. As the metal moved towards the centre of the cavity the conformation changed from *tt* to *gg*. However, this did not

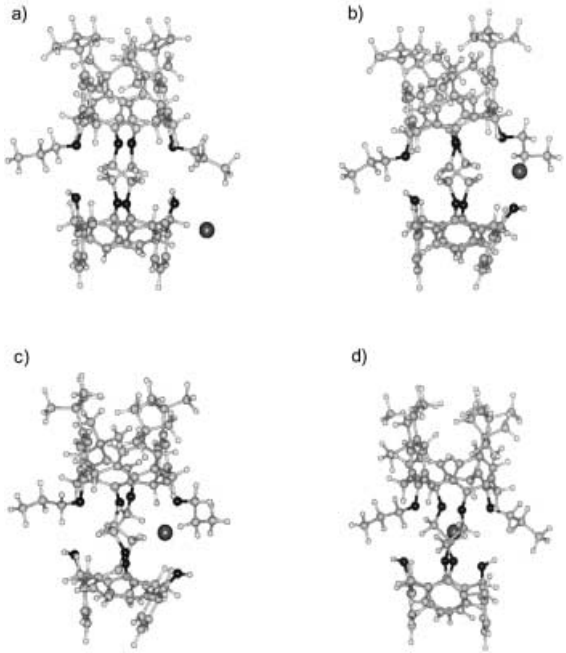

Figure 7. Snapshots at various times during the molecular dynamics simulation of the formation of $\mathbf{9}\cdot K^+$ showing how the metal ion enters the cavity by the horizontal route. Snapshots are taken after a) 210.0, b) 215.6, c) 216.3 and d) 216.6 ps.

happen until the metal was within 2 Å of the centre of the cavity. It is apparent from Figure 7, that as the metal approaches the cavity, the terminal ether group acts as a flap, opening to allow the metal ion to enter the cavity and then closing once the metal is enclosed.

Subsequent simulations showed that the metal ion could enter the cavity by the two vertical routes, but only when the temperature was increased to 500 K. It is interesting to note that when the metal follows the vertical route there is no specific conformational change as is observed in the calix[4]-tube. Instead we find in a typical simulation that the metal reaches the plane at the bottom of the phenyl rings while the conformation is still *tt*, one torsion angle changes to *gauche* as the metal approaches the plane of the four oxygen atoms at the bottom of the cone and it is only when the metal enters the cavity that the conformation changes to *gg*.

It is interesting that with the calix[4]tube, the reaction path was successfully followed by the K^+ ion at 400 K. These results confirm that the metal ion readily enters the cavity of **9** by the horizontal path and the results are consistent with the experimental results that the metal complexes with **9** more readily than with the calix[4]tube.

Conclusion

The new calix[4]semitube ligand design consisting of two calix[4]arene units linked by two ethylene groups, together with 1,3-disubstituted propyl ether and phenolic −OH functional groups creating eight oxygen donor sites, represents a new class of ionophore that exhibits remarkable selectivity for potassium together with fast complexation kinetics. This is contrary to the slow kinetics of binding exhibited by the potassium selective calix[4]tube.

Molecular modelling simulations, on structural models from crystallographic determinations, demonstrate that the most likely route of entry for the potassium cation into the calix[4]semitube is through a horizontal or "side-on" route, which contrasts with the preferred vertical pathway through the calix[4]arene annulus of the calix[4]tube. This horizontal mode of potassium cation entry may account for the calix[4]semitube exhibiting fast kinetics of complexation relative to those of the calix[4]tube. The length of the bridging alkylene chain between the respective calix[4]arenes of the calix[4]semitube crucially dictates the strength and selectivity of alkali metal cation binding.

Experimental Section

General: All chemicals were commercial grade and used without further purification unless stated otherwise. Solvents were predried, purified by distillation and stored under nitrogen where appropriate. Acetonitrile and dichloromethane were distilled from calcium hydride, tetrahydrofuran from sodium wire with benzophenone as an indicator and triethylamine was distilled from potassium hydroxide. Prior to use, pyridine was dried over potassium hydroxide and dimethylformamide was dried over molecular sieves (4 Å).

NMR spectra were recorded by using either a 300 MHz Varian VXWorks spectrometer or a 500 MHz Varian Unity spectrometer. Electrospray mass spectra were recorded by using Micromass LCT equipment. Microanalyses were obtained on an elementar vario EL and were performed by the Inorganic Chemistry Laboratory, University of Oxford.

p-tert-Butylcalix[4]arene,[14] calix[4]arene[15] and 1,3-dipropoxy-*tert*-butylcalix[4]arene (**1**)[16] were prepared according to literature procedures.

5,11,17,23-Tetra-*tert*-butyl-25,27-bis[(ethoxycarbonyl)methoxy]-26,28-dipropoxycalix[4]arene (2): A solution of **1** (5.0 g, 6.82 mmol) and NaH (1.63 g, 40 mmol) in tetrahydrofuran (125 mL) was stirred at room temperature for 1 hour then ethyl bromoacetate (6.68 g, 4.44 mL, 40 mmol) was added. Following a further 72 hours stirring, water (50 mL) was added dropwise. The organic solvent was then removed in vacuo and the aqueous layer extracted with dichloromethane (3×50 mL). The combined organic extracts were dried ($MgSO_4$) and reduced in vacuo yielding a brown oil. By recrystallising from methanol/dichloromethane in the fridge, pure **2** was obtained as a white powder (5.23 g, 85 %). ^{1}H NMR (500 MHz, [D]$CHCl_3$, 18 °C): $\delta = 1.00$ (t, $^3J(H,H) = 7.4$ Hz, 6H; $OCH_2CH_2CH_3$), 1.01 (s, 18H; $(CH_3)_3C$), 1.14 (s, 18H; $(CH_3)_3C$), 1.28 (t, $^3J(H,H) = 7.1$ Hz, 6H; $C(O)OCH_2CH_3$), 1.95 (m, 4H; $OCH_2CH_2CH_3$), 3.17 (d, $^2J(H,H) = 12.8$ Hz, 4H; $ArCH_2Ar$), 3.82 (t, $^3J(H,H) = 7.5$ Hz, 4H; $OCH_2CH_2CH_3$), 4.21 (q, $^3J(H,H) = 7.1$ Hz, 4H; $C(O)OCH_2CH_3$), 4.62 (d, $^2J(H,H) = 12.8$ Hz, 4H; $ArCH_2Ar$), 4.79 (s, 4H; $OCH_2C(O)$), 6.68 (s, 4H; ArH), 6.86 ppm (s, 4H; ArH); ^{13}C NMR (75 MHz, [D]$CHCl_3$, 18 °C): $\delta = 10.44$ ($OCH_2CH_2CH_3$), 14.18 (OCH_2CH_3), 23.21 ($OCH_2CH_2CH_3$), 31.32 ($(CH_3)_3C$), 31.44 ($(CH_3)_3C$), 31.62 ($ArCH_2Ar$), 33.70 ($(CH_3)_3C$), 33.85 ($(CH_3)_3C$), 60.33 (OCH_2CH_3), 70.76 and 77.04 ($OCH_2CH_2CH_3$ and $OCH_2C(O)$), 124.80, 125.34, 133.09, 133.98, 144.28, 144.91, 152.90 and 153.57 (Ar), 170.47 ppm (C=O); MS (ES): *m*/*z*: 928 [M^++Na], 944 [M^++K]; elemental analysis calcd (%) for $C_{58}H_{80}O_8$: C 76.95, H 8.91; found: C 76.75, H 9.81.

5,11,17,23-Tetra-*tert*-butyl-25,27-bis[(ethoxycarbonyl)propoxy]-26,28-dipropoxycalix[4]arene (3): Calix[4]arene **1** (2.0 g, 2.73 mmol) and NaH (0.66 g, 16.4 mmol) were stirred in dimethylformamide (75 mL) at room temperature for 2 hours. After this time, ethyl-4-bromobutyrate (3.20 g, 16.4 mmol) was added and stirring continued for a further 48 hours. Following removal of the solvent in vacuo, the mixture was partitioned between dichloromethane (75 mL) and water (75 mL). The organic layer was then washed with saturated NH_4Cl (75 mL), dried ($MgSO_4$) and reduced in vacuo. The residue was purified by column chromatography on silica gel eluting with 3:2 (v/v) chloroform:hexane. The fastest moving fraction was collected and reduced in vacuo giving **3** as a white powder (1.20 g, 46 %). ^{1}H NMR (500 MHz, [D]$CHCl_3$, 18 °C): $\delta = 1.00$ (t, $^3J(H,H) = 7.5$ Hz, 6H; $OCH_2CH_2CH_3$), 1.07 (s, 18H; $(CH_3)_3C$), 1.12 (s, 18H; $(CH_3)_3C$), 1.29 (t, $^3J(H,H) = 7.0$ Hz, 6H; $C(O)OCH_2CH_3$), 2.03 (m, 4H; $OCH_2CH_2CH_3$), 2.33 (m, 4H; $OCH_2CH_2CH_2C(O)$), 2.52 (t, $^3J(H,H) = 7.5$ Hz, 4H; $OCH_2CH_2CH_2C(O)$), 3.14 (d, $^2J(H,H) = 12.5$ Hz, 4H; $ArCH_2Ar$), 3.82 (t, $^3J(H,H) = 7.5$ Hz, 4H; $OCH_2CH_2CH_3$), 3.91 (t, $^3J(H,H) = 7.5$ Hz, 4H; $OCH_2CH_2CH_2C(O)$), 4.17 (q, $^3J(H,H) = 7.0$ Hz, 4H; $C(O)OCH_2CH_3$), 4.39 (d, $^2J(H,H) = 12.5$ Hz, 4H; $ArCH_2Ar$), 6.76 (s, 4H; ArH), 6.82 ppm (s, 4H; ArH); ^{13}C NMR (125 MHz, [D]$CHCl_3$, 18 °C): $\delta = 10.25$ ($OCH_2CH_2CH_3$), 14.26 ($C(O)OCH_2CH_3$), 23.29 ($OCH_2CH_2CH_2C(O)$), 25.54 ($OCH_2CH_2CH_3$), 31.01 and 31.22 ($ArCH_2Ar$ and $OCH_2CH_2CH_2C(O)$), 31.40 ($(CH_3)_3C$), 31.45 ($(CH_3)_3C$), 33.77 ($(CH_3)_3C$), 33.81 ($(CH_3)_3C$), 60.24 ($C(O)OCH_2CH_3$), 74.11 ($OCH_2CH_2CH_2C(O)$), 77.04 ($OCH_2CH_2CH_3$), 124.86, 124.98, 133.52, 133.87, 144.20, 144.47 and 153.39 (coincident) (Ar), 173.41 ppm ($O(CH_2)_3C(O)$); MS (ES): *m*/*z*: 979 [M^++NH_4], 984 [M^++Na]; elemental analysis calcd (%) for $C_{62}H_{88}O_8$: C 77.46, H 9.23; found: C 77.33, H 9.43.

5,11,17,23-Tetra-*tert*-butyl-25,27-bis(hydroxyethoxy)-26,28-dipropoxycalix[4]arene (4): $LiAlH_4$ (1.24 g, 33 mmol) was added in small portions at 0 °C to a solution of calix[4]arene bis(ester) **2** (5.95 g, 6.57 mmol) in tetrahydrofuran (150 mL). The reaction mixture was allowed to warm to room temperature and then left to stir overnight. Following careful addition of 2 M H_2SO_4 (50 mL), the mixture was left to stir for a further hour. The organic solvent was removed in vacuo and the aqueous layer extracted with dichloromethane (2×125 mL). The combined organic extracts were then dried ($MgSO_4$) and reduced in vacuo. If necessary, the product can be recrystallised from methanol/dichloromethane in the fridge to yield pure **4** as large colourless crystals (4.56 g, 85 %). ^{1}H NMR (500 MHz, [D]$CHCl_3$, 18 °C): $\delta = 0.84$ (s, 18H; $(CH_3)_3C$), 0.95 (t, $^3J(H,H) = 7.5$ Hz, 6H; $OCH_2CH_2CH_3$), 1.36 (s, 18H; $(CH_3)_3C$), 1.88 (m, 4H; $OCH_2CH_2CH_3$), 3.20 (d, $^2J(H,H) = 12.5$ Hz, 4H; $ArCH_2Ar$), 3.74 (t, $^3J(H,H) = 7.5$ Hz, 4H; $OCH_2CH_2CH_3$), 4.03 (m, 4H; OCH_2CH_2OH), 4.12

(m, 4H; OCH_2CH$_2$OH), 4.36 (d, ^2J(H,H) = 12.5 Hz, 4H; ArCH_2Ar), 5.09 (brs, 2H; OH), 6.50 (s, 4H; ArH), 7.16 ppm (s, 4H; ArH); ^{13}C NMR (75 MHz, [D]CHCl$_3$, 18 °C): δ = 10.15 (OCH$_2$CH$_2$*C*H$_3$), 22.52 (OCH$_2$*C*H$_2$CH$_3$), 30.77 (Ar*C*H$_2$Ar), 31.06 ((*C*H$_3$)$_3$C), 31.69 ((*C*H$_3$)$_3$C), 33.59 ((CH$_3$)$_3$*C*), 34.09 ((CH$_3$)$_3$*C*), 61.65, 76.90 and 78.46 (O*C*H$_2$CH$_2$CH$_3$, O*C*H$_2$CH$_2$OH and OCH$_2$*C*H$_2$OH), 124.71, 125.80, 131.75, 135.55, 144.62, 145.58, 151.16 and 153.76 ppm (Ar); MS (ES): *m*/*z*: 844 [*M*$^+$+Na], 860 [*M*$^+$+K]; elemental analysis calcd (%) for C$_{54}$H$_{76}$O$_6$: C 78.98, H 9.33; found: C 78.73, H 10.32.

5,11,17,23-Tetra-*tert*-butyl-25,27-bis(hydroxybutoxy)-26,28-dipropoxycalix[4]arene (5): LiAlH$_4$ (0.16 g, 4.16 mmol) was added in small portions at 0 °C to a solution of calix[4]arene bis(ester) **3** (1.0 g, 1.04 mmol) in tetrahydrofuran (40 mL). The mixture was then allowed to stir overnight at room temperature. After careful addition of 2 M H$_2$SO$_4$ (40 mL) and a further hour of stirring, the tetrahydrofuran was removed in vacuo. The aqueous layer was then extracted with dichloromethane (2 × 50 mL). The combined organic extracts were subsequently dried (MgSO$_4$) and reduced in vacuo. Pure **5** could be precipitated from methanol/water as a white powder (0.79 g, 87%). ^{1}H NMR (500 MHz, [D]CHCl$_3$, 18 °C): δ = 0.99 (s, 18H; (CH$_3$)$_3$C), 1.03 (t, ^3J(H,H) = 7.5 Hz, 6H; OCH$_2$CH$_2$C*H*$_3$), 1.19 (s, 18H; (CH$_3$)$_3$C), 1.67 (m, 4H; O(CH$_2$)$_2$C*H*$_2$CH$_2$OH), 1.98 (m, 4H; OCH$_2$C*H*$_2$CH$_3$), 2.15 (m, 4H; OCH$_2$C*H*$_2$(CH$_2$)$_2$OH), 3.13 (d, ^2J(H,H) = 13.0 Hz, 4H; ArC*H*$_2$Ar), 3.76 (m, 8H; OC*H*$_2$CH$_2$CH$_3$ and O(CH$_2$)$_3$C*H*$_2$OH coincident), 3.96 (t, ^3J(H,H) = 7.5 Hz, 4H; OC*H*$_2$(CH$_2$)$_3$OH), 4.41 (d, ^2J(H,H) = 13.0 Hz, 4H; ArC*H*$_2$Ar), 6.66 (s, 4H; Ar), 6.91 ppm (s, 4H; Ar); ^{13}C NMR (75 MHz, [D]CHCl$_3$, 18 °C): δ = 10.65 (OCH$_2$CH$_2$*C*H$_3$), 23.51, 26.55 and 29.43 (OCH$_2$*C*H$_2$CH$_3$, OCH$_2$*C*H$_2$(CH$_2$)$_2$OH and O(CH$_2$)$_2$*C*H$_2$CH$_2$OH), 31.14 (Ar*C*H$_2$Ar), 31.39 ((*C*H$_3$)$_3$C), 31.62 ((*C*H$_3$)$_3$C), 33.75 ((CH$_3$)$_3$*C*), 33.95 ((CH$_3$)$_3$*C*), 62.96 (O(CH$_2$)$_3$*C*H$_2$OH), 74.83 (O*C*H$_2$(CH$_2$)$_3$OH), 77.17 (O*C*H$_2$CH$_2$CH$_3$), 124.62, 125.05, 132.91, 134.43, 143.99, 144.38, 153.09 and 153.86 ppm (Ar); MS (ES): *m*/*z*: 895 [*M*$^+$+NH$_4$], 900 [*M*$^+$+Na]; elemental analysis calcd (%) for C$_{62}$H$_{88}$O$_8$: C 79.41, H 9.65; found: C 79.20, H 9.68.

5,11,17,23-Tetra-*tert*-butyl-25,27-bis(tosylethoxy)-26,28-dipropoxycalix[4]arene (6): *para*-Toluenesulphonyl chloride (10.7 g, 56 mmol) was added in one portion to a stirred solution of calix[4]arene bis(alcohol) **4** (4.6 g, 5.6 mmol) in pyridine (60 mL) and the mixture was stirred for 30 minutes. The flask was then refrigerated at around 4 °C for 5 days after which time the red solution was poured into iced 2 M HCl (200 mL). The precipitate was filtered, taken up in chloroform (150 mL) and washed with water (200 mL). The organic layer was dried (MgSO$_4$) and reduced in vacuo. Pure **6** was obtained as large colourless crystals (5.49 g, 87%) by crystallisation from methanol (75 mL). ^{1}H NMR (300 MHz, [D]CHCl$_3$, 18 °C): δ = 0.85 (s, 18H; (CH$_3$)$_3$C), 0.93 (t, ^3J(H,H) = 7.2 Hz, 6H; OCH$_2$CH$_2$C*H*$_3$), 1.30 (s, 18H; (CH$_3$)$_3$C), 1.79 (m, 4H; OCH$_2$C*H*$_2$CH$_3$), 2.48 (s, 6H; Ts-C*H*$_3$), 3.08 (d, ^2J(H,H) = 12.9 Hz, 4H; ArC*H*$_2$Ar), 3.62 (t, ^3J(H,H) = 7.5 Hz, 4H; OC*H*$_2$CH$_2$CH$_3$), 4.23 (d, ^2J(H,H) = 12.9 Hz, 4H; ArC*H*$_2$Ar), 4.24 (t, ^3J(H,H) = 6.0 Hz, 4H; OCH$_2$C*H*$_2$OTs), 4.63 (t, ^3J(H,H) = 6.0 Hz, 4H; OC*H*$_2$CH$_2$OTs), 6.48 (s, 4H; ArH), 7.02 (s, 4H; ArH), 7.37 (d, ^3J(H,H) = 8.1 Hz, 4H; Ts-ArH), 7.81 ppm (d, ^3J(H,H) = 8.1 Hz, 4H; Ts-ArH); ^{13}C NMR (75 MHz, [D]CHCl$_3$, 18 °C): δ = 10.50 (OCH$_2$CH$_2$*C*H$_3$), 21.72 (Ts-*C*H$_3$), 23.29 (OCH$_2$*C*H$_2$CH$_3$), 31.09 (Ar*C*H$_2$Ar), 31.17 ((*C*H$_3$)$_3$C), 31.68 ((*C*H$_3$)$_3$C), 33.62 ((CH$_3$)$_3$*C*), 34.09 ((CH$_3$)$_3$*C*), 69.03 and 70.62 (OCH$_2$-CH$_2$OTs and OCH$_2$*C*H$_2$OTs), 77.63 (O*C*H$_2$CH$_2$CH$_3$), 124.52, 125.37, 127.78, 129.74, 131.89, 133.41, 134.90, 144.14, 144.47, 145.42, 152.13 and 153.22 ppm (Ar and Ts-Ar); MS (ES): *m*/*z*: 1153 [*M*$^+$+Na], 1169 [*M*$^+$+K]; elemental analysis calcd (%) for C$_{68}$H$_{88}$O$_{10}$S$_2$ · H$_2$O: C 71.17, H 7.90; found: C 70.96, H 8.11.

5,11,17,23-Tetra-*tert*-butyl-25,27-bis(tosylbutoxy)-26,28-dipropoxycalix[4]arene (7): Triethylamine (3 mL, 21 mmol) and *para*-toluenesulphonyl chloride (0.76 g, 4.0 mmol)was added to a solution of calix[4]arene bis(alcohol) **5** (0.70 g, 0.80 mmol) in dichloromethane (20 mL). The mixture was stirred at room temperature for 42 hours. Water (20 mL) was then added and stirring continued for a further 0.5 hours. The organic layer was washed with 2 M HCl (2 × 50 mL) and saturated NaCl solution (50 mL), dried (MgSO$_4$) and then reduced in vacuo. Reprecipitation from ethanol/water gave pure **7** as a white powder (0.58 g 61%). ^{1}H NMR (500 MHz, [D]CHCl$_3$, 18 °C): δ = 0.94 (t, ^3J(H,H) = 7.5 Hz, 6H; OCH$_2$CH$_2$C*H*$_3$), 1.05 (s, 18H; (CH$_3$)$_3$C), 1.11 (s, 18H; (CH$_3$)$_3$C), 1.80 (m, 4H; OCH$_2$C*H*$_2$(CH$_2$)$_2$OTs), 1.92 (m, 4H; OCH$_2$C*H*$_2$CH$_3$), 2.02 (m, 4H; O(CH$_2$)$_2$C*H*$_2$CH$_2$OTs), 2.45 (s, 6H; Ts-C*H*$_3$), 3.09 (d, ^2J(H,H) = 12.5 Hz, 4H; ArC*H*$_2$Ar), 3.74 (t, ^3J(H,H) = 7.5 Hz, 4H; OC*H*$_2$CH$_2$CH$_3$), 3.82 (t, ^3J(H,H) = 7.5 Hz, 4H; O(CH$_2$)$_3$C*H*$_2$OTs), 4.10 (t, ^3J(H,H) = 6.5 Hz, 4H; OC*H*$_2$(CH$_2$)$_3$OTs), 4.30 (d, ^2J(H,H) = 12.5 Hz, 4H; ArC*H*$_2$Ar), 6.73 (s, 4H; ArH), 6.80 (s, 4H; ArH), 7.36 (d, ^3J(H,H) = 7.5 Hz, 4H; Ts-ArH), 7.81 ppm (d, ^3J(H,H) = 7.5 Hz, 4H; Ts-ArH); ^{13}C NMR (75 MHz, [D]CHCl$_3$, 18 °C): δ = 10.40 (OCH$_2$CH$_2$*C*H$_3$), 21.70 (Ts-*C*H$_3$), 23.44, 25.84 and 26.24 (OCH$_2$*C*H$_2$CH$_3$, OCH$_2$*C*H$_2$(CH$_2$)$_2$OTs and O(CH$_2$)$_2$*C*H$_2$CH$_2$OTs), 31.09 (Ar*C*H$_2$Ar), 31.46 ((*C*H$_3$)$_3$C), 31.50 ((*C*H$_3$)$_3$C), 33.81 ((CH$_3$)$_3$*C*), 33.88 ((CH$_3$)$_3$*C*), 70.44 (O(CH$_2$)$_3$*C*H$_2$OTs), 74.03 (O*C*H$_2$(CH$_2$)$_3$OTs), ca.77 under solvent (O*C*H$_2$CH$_2$CH$_3$), 124.79, 124.93, 127.79, 129.78, 133.07, 133.32, 133.74, 144.17, 144.48, 144.60 and 153.24 ppm (2 coincident) (Ar and Ts-Ar); MS (ES): *m*/*z*: 1209 [*M*$^+$+Na], 1225 [*M*$^+$+K]; elemental analysis calcd (%) for C$_{72}$H$_{96}$O$_{10}$S$_2$: C 72.94, H 8.16; found: C 72.66, H, 8.22.

***tert*-Butyl ethyl semitube (8)**: A suspension of *p*-*tert*-butylcalix[4]arene (0.58 g, 0.89 mmol) and K$_2$CO$_3$ (1.23 g, 8.9 mmol) was refluxed in acetonitrile (50 mL) for 2.5 hours. After this time, the bis(tosyl) substituted calix[4]arene **6** (1.0 g, 0.89 mmol) was added and the mixture was refluxed for a further 7–10 days. Following removal of the solvent in vacuo, the mixture was partitioned between chloroform (50 mL) and water (50 mL). The organic layer was dried (MgSO$_4$) and reduced in vacuo. Ethanol (75 mL) was added to this crude material, which after briefly refluxing, was hot-filtered giving **8** as a white powder (0.68 g, 53%). ^{1}H NMR (500 MHz, [D]CHCl$_3$, 18 °C): δ = 0.62 (t, ^3J(H,H) = 7.2 Hz, 6H; OCH$_2$CH$_2$C*H*$_3$), 0.84 (s, 18H; (CH$_3$)$_3$C), 1.21 (s, 36H; 2 × [(CH$_3$)$_3$C)] (coincident)), 1.36 (s, 18H; (CH$_3$)$_3$C), 1.71 (m, 4H; OCH$_2$C*H*$_2$CH$_3$), 3.25 (d, ^2J(H,H) = 12.9 Hz, 4H; ArC*H*$_2$Ar), 3.43 (d, ^2J(H,H) = 13.5 Hz, 4H; ArC*H*$_2$Ar), 3.95 (t, ^3J(H,H) = 7.8 Hz, 4H; OC*H*$_2$CH$_2$CH$_3$), 4.56 (d, ^2J(H,H) = 12.3 Hz, 4H; ArC*H*$_2$Ar), 4.60 (d, ^2J(H,H) = 12.3 Hz, 4H; ArC*H*$_2$Ar), 5.10 (t, ^3J(H,H) = 7.8 Hz, 4H; ROC*H*$_2$CH$_2$OR′), 5.28 (t, ^3J(H,H) = 7.8 Hz, 4H; ROCH$_2$C*H*$_2$OR′), 6.42 (s, 4H; ArH), 6.99 (s, 4H; ArH), 7.07 (s, 4H; ArH), 7.12 (s, 4H; ArH), 9.29 ppm (s, 2H; OH); ^{13}C NMR (75 MHz, [D]CHCl$_3$, 18 °C): δ = 10.07 (OCH$_2$CH$_2$*C*H$_3$), 22.77 (OCH$_2$*C*H$_2$CH$_3$), 31.18, 31.29, 31.56 and 31.72 ((*C*H$_3$)$_3$C), 32.26, 33.56, 33.87, 33.92, 34.01 and 34.02 ((CH$_3$)$_3$*C* and 2 × [Ar*C*H$_2$Ar]), 71.05, 73.54 and 77.49 (O*C*H$_2$), 124.12, 125.16, 125.68, 126.45, 128.45, 131.56, 132.81, 134.96, 141.56, 143.70, 144.58, 146.26, 150.41, 150.76, 153.33 and 154.61 ppm (Ar); MS (ES): *m*/*z*: 1457 [*M*$^+$+Na], 1473 [*M*$^+$+K]; elemental analysis calcd (%) for C$_{98}$H$_{128}$O$_8$ · 1/3(CHCl$_3$): C 80.13, H 8.78; found: C 80.53, H 8.61.

De-*tert*-butyl ethyl semitube (9): A suspension of calix[4]arene (0.38 g, 0.89 mmol) and K$_2$CO$_3$ (1.23 g, 8.9 mmol) was refluxed in acetonitrile (50 mL) for 2 hours. After this time, the bis(tosyl) substituted calix[4]arene **6** (1.0 g, 0.89 mmol) was added and the mixture was refluxed for a further 9.5 days. Following removal of the solvent in vacuo, the mixture was partitioned between chloroform (100 mL) and water (100 mL). The organic layer was dried (MgSO$_4$) and reduced in vacuo. Ethanol (50 mL) was added to this pink/brown solid which after briefly refluxing, was hot-filtered giving **9** as a white powder (0.52 g). A further small crop of desired product (0.08 g) could be obtained by loading the remaining residue onto a silica gel column and gradient eluting from dichloromethane to 10% ethyl acetate to 10% methanol. Combined yield (0.60 g, 56%). ^{1}H NMR (500 MHz, [D]CHCl$_3$, 18 °C): δ = 0.57 (t, ^3J(H,H) = 7.5 Hz, 6H; OCH$_2$CH$_2$C*H*$_3$), 0.82 (s, 18H; (CH$_3$)$_3$C), 1.34 (s, 18H; (CH$_3$)$_3$C), 1.70 (m, 4H; OCH$_2$C*H*$_2$CH$_3$), 3.26 (d, ^2J(H,H) = 13.0 Hz, 4H; ArC*H*$_2$Ar), 3.47 (d, ^2J(H,H) = 13.0 Hz, 4H; ArC*H*$_2$Ar), 3.91 (t, ^3J(H,H) = 8.0 Hz, 4H; OC*H*$_2$CH$_2$CH$_3$), 4.55 (d, ^2J(H,H) = 13.0 Hz, 4H; ArC*H*$_2$Ar), 4.60 (d, ^2J(H,H) = 12.5 Hz, 4H; ArC*H*$_2$Ar), 5.14 (t, ^3J(H,H) = 7.3 Hz, 4H; ROC*H*$_2$CH$_2$OR′), 5.31 (t, ^3J(H,H) = 7.3 Hz, 4H; ROCH$_2$C*H*$_2$OR′), 6.44 (s, 4H; ArH), 6.61 (t, ^3J(H,H) = 7.5 Hz, 2H; ArH), 6.80 (t, ^3J(H,H) = 7.5 Hz, 2H; ArH), 7.03 (d, ^3J(H,H) = 7.5 Hz, 2H; ArH), 7.07 (d, ^3J(H,H) = 7.5 Hz, 2H; ArH), 7.16 (s, 4H; ArH), 9.44 ppm (s, 2H; OH); ^{13}C NMR (75 MHz, [D]CHCl$_3$, 18 °C): δ = 10.06 (OCH$_2$CH$_2$*C*H$_3$), 22.91 (OCH$_2$*C*H$_2$CH$_3$), 31.16 ((*C*H$_3$)$_3$C), 31.71 ((*C*H$_3$)$_3$C), 32.18, 33.04, 33.56 and 34.04 ((CH$_3$)$_3$*C* and 2?[Ar*C*H$_2$Ar]), 71.37, 73.78 and 77.62 (O*C*H$_2$), 119.52, 124.18, 124.53, 125.76, 128.22, 128.88, 129.56, 131.49, 133.27, 134.92, 143.80, 144.72, 152.36, 152.77, 153.27 and 154.59 ppm (Ar); MS (ES): *m*/*z*: 1249 [*M*$^+$+K]; elemental analysis calcd (%) for C$_{82}$H$_{96}$O$_8$.1/3(CHCl$_3$): C 79.17, H 7.77; found: C 79.21, H 7.47.

***tert*-Butyl butyl semitube (10)**: A suspension of *p*-*tert*-butylcalix[4]arene (0.091 g, 0.14 mmol) and K$_2$CO$_3$ (0.077 g, 0.56 mmol) was refluxed in acetonitrile (50 mL) for 2 hours. After this time, bis(tosyl) substituted calix[4]arene **7** (0.20 g, 0.17 mmol) was added and the mixture refluxed for a further 5 days. Following removal of the solvent in vacuo, the mixture was

partitioned between chloroform (75 mL) and water (75 mL). The organic layer was dried ($MgSO_4$) and reduced in vacuo. The residue was heated in acetonitrile (20 mL) and the solid hot-filtered giving pure **10** as a white solid (0.149 g, 71 %). ^{1}H NMR (500 MHz, [D]CHCl$_3$, 18 °C): $\delta = 0.60$ (t, ^3J(H,H) = 7.5 Hz, 6H; $OCH_2CH_2CH_3$), 0.83 (s, 18H; $(CH_3)_3C$), 1.10 (s, 18H; $(CH_3)_3C$), 1.25 (s, 18H; $(CH_3)_3C$), 1.36 (s, 18H; $(CH_3)_3C$), 1.68 (m, 4H; $OCH_2CH_2CH_3$), 2.12 and 2.66 (m, 8H; $ROCH_2CH_2(CH_2)_2OR'$ and $RO(CH_2)_2CH_2CH_2OR'$), 3.15 (d, ^2J(H,H) = 13.0 Hz, 4H; $ArCH_2Ar$), 3.36 (d, ^2J(H,H) = 13.0 Hz, 4H; $ArCH_2Ar$), 3.71 (t, ^3J(H,H) = 7.5 Hz, 4H; $OCH_2CH_2CH_3$), 4.07 (t, ^3J(H,H) = 5.0 Hz, 4H; $RO(CH_2)_3CH_2OR'$), 4.32 (t, ^3J(H,H) = 7.5 Hz, 4H; $ROCH_2(CH_2)_3OR'$), 4.37 (d, ^2J = 13.0 Hz, 4H; $ArCH_2Ar$), 4.52 (d, ^2J(H,H) = 13.0 Hz, 4H; $ArCH_2Ar$), 6.43 (s, 4H; ArH), 6.97 (s, 4H; ArH), 7.03 (s, 4H; ArH), 7.14 (s, 4H; ArH), 8.46 ppm (s, 2H; OH); ^{13}C NMR (75 MHz, [D]CHCl$_3$, 18 °C): $\delta = 9.95$ ($OCH_2CH_2CH_3$), 22.90 ($OCH_2CH_2CH_3$), 27.25, 28.17, 29.76 and 32.23 (2 × [$ArCH_2Ar$] and $ROCH_2CH_2CH_2CH_2OR'$), 31.20, 31.26, 31.72 and 31.82 (($CH_3)_3C$), 33.61, 33.82, 34.09 and 34.11 (($(CH_3)_3C$)), 75.32 and 77.24 ($OCH_2CH_2CH_3$, $ROCH_2(CH_2)_3OR'$ and $RO(CH_2)_3CH_2OR'$ (coincident)), 124.08, 125.05, 125.46, 125.56, 127.62, 131.82, 133.11, 135.53, 141.18, 143.51, 144.30, 146.72, 149.86, 150.82, 152.48 and 155.12 ppm (Ar); MS (ES): *m*/*z*: 1508 [M^++NH_4], 1513 [M^++Na]; elemental analysis calcd (%) for $C_{102}H_{136}O_8$.1/2($CHCl_3$): C 79.43, H 8.88; found: C 79.49, H 9.00.

Computational methods: All simulations were carried out in the gas phase. Molecular dynamics were carried out at a variety of temperatures by using the Cerius2 software package[17] with parameters from the Universal Force Field.[18] Partial atomic charges for atoms in the calix[4]semitube were calculated by using the Gasteiger method implemented in Cerius2. The atoms in the O-CH_2-CH_2-O links were given charges taken from ref. [19] and the charges on the rest of the molecule were then adjusted to give a neutral tube. The step size was 1.0 fs and the simulations were carried out for 500 ps. The set of atomic positions were saved every 100 time steps (0.10 ps) leading to trajectory files with 5000 conformations collected over 500 ps. A constant NVE thermostat with default parameters was used. Simulations were carried out with K^+ at several different temperatures. In these simulations the metals were given a +1 charge and the charges on the calix[4]semitube were kept unchanged.

Stability constant determinations: As cation complexation/decomplexation with **8** and **9** was slow on the NMR timescale, stability constants could be assessed by direct integration of the host and complex resonances. For both ligands, spectra were recorded in the presence of various equivalents of each cation (in the range of 0 to 5 equivalents). A *K* value was calculated for each spectrum recorded. The quoted stability constant for each ligand/cation system is the average of these *K* values.

Crystallographic measurements: Crystal data for **4**: $C_{54}H_{76}O_6$, $M_r = 821.15$, monoclinic, $P2_1/c$, $a = 15.84(2)$, $b = 15.74(2)$, $c = 20.22(3)$ Å, $\beta = 94.94(1)°$, $V = 5021$ Å^3, $Z = 4$, $\rho_{calcd} = 1.086$ Mg m^{-3}. Intensity data were collected with $Mo_{K\alpha}$ radiation using the *MAR*research image plate system. The crystal was positioned at 70 mm from the image plate. A total of 100 frames were measured at 2° intervals with a counting time of 4 mins to give 8934 independent reflections. Data analysis was carried out with the XDS program.[20] The structure was solved by using direct methods with the SHELX86 program.[21] All non-hydrogen atoms were refined with anisotropic thermal parameters. The hydrogen atoms were included in geometric positions and given thermal parameters equivalent to 1.2 times those of the atom to which they were attached. The structure was refined on F^2 using SHELXL.[22] The final *R* values were $R_1 = 0.0912$ and $wR_2 = 0.2564$ for 4459 data with $I > 2\sigma(I)$.

Crystal data for **9**·$CHCl_3$: $C_{83}H_{97}Cl_3O_8$, $M_r = 1329.04$, monoclinic, $P2_1/c$, $a = 21.4788(1)$, $b = 16.8308(1)$, $c = 21.8377(1)$ Å, $\beta = 113.3191(3)°$, $V = 7249.6$ Å^3, $Z = 4$, $\rho_{calcd} = 1.218$ Mg m^{-3}. Data was obtained by using $Mo_{K\alpha}$ radiation on an Enraf-Nonius KappaCCD diffractometer. Crystals were mounted on a glass fibre and cooled rapidly to 150 K in a stream of cold N_2 using an Oxford Cryosystems CRYOSTREAM unit. Intensity data were processed using the DENZO-SMN package.[23] Structures were solved by direct methods by using the SIR92 program.[24] Full-matrix least-squares refinement on *F* was carried out using the CRYSTALS program suite.[25] Hydrogen atoms were positioned geometrically after each cycle of refinement. A Chebychev polynomial weighting scheme was applied. The final *R* values were $R_1 = 0.0728$ and $wR_2 = 0.0857$ for 11977 data with $I > 2\sigma(I)$.

CCDC 195350 and 195351 contain(s) the supplementary crystallographic data for this paper. These data can be obtained free of charge via www.ccdc.cam.ac.uk/conts/retrieving.html (or from the Cambridge Crystallographic Data Centre, 12 Union Road, Cambridge CB2 1EZ, UK; fax: (+44) 1223-336-033; or e-mail: deposit@ccdc.cam.ac.uk).

Acknowledgement

We thank the EPSRC for a studentship (PRAW) and the EPSRC and University of Reading for funds for the crystallographic image plate system.

[1] A. Ikeda, S. Shinkai, *Chem. Rev.* **1997**, *97*, 1713; P. D. Beer, P. A. Gale, Z. Chen, *Adv. Phys. Org. Chem.* **1998**, *31*, 1; X. X. Zhang, R. M. Izatt, J. S. Bradshaw, K. E. Krakowiak, *Coord. Chem. Rev.* **1998**, *174*, 179.
[2] D. A. Doyle, J. M. Cabral, R. A. Pfuetzner, A. Kuo, J. M. Gulbis, S. L. Cohen, B. T. Chait, R. MacKinnon, *Science* **1998**, *280*, 69.
[3] G. W. Gokel, *Chem. Commun.* **2000**, 1; J. de Mendoza, F. Cuevas, P. Prados, E. S. Meadows, G. W. Gokel, *Angew. Chem.* **1998**, *110*, 1650; *Angew. Chem. Int. Ed.* **1998**, *37*, 1534; Y. Tanake, Y. Kobuke, M. Sokabe, *Angew. Chem.* **1995**, *107*, 717; *Angew. Chem Int. Ed. Engl.* **1995**, *34*, 693.
[4] For general reviews on calixarenes, see: C. D. Gutsche, *Calixarenes*, The Royal Society of Chemistry, Cambridge, (UK), **1989**; V. Böhmer, *Angew. Chem.* **1995**, *34*, 785; *Angew. Chem. Int. Ed. Engl.* **1995**, *34*, 713.
[5] K. Iwamoto, S. Shinkai, *J. Org. Chem.* **1992**, *116*, 3102.
[6] A. Cadogan, D. Diamond, S. Cremin, M. A. McKervey, S. J. Harris, *Anal. Proc.* **1991**, *28*, 13.
[7] W. H. Chan, A. W. M. Lee, D. W. J. Kwong, W. L. Tam, K.-M Wang, *Analyst* **1996**, *121*, 531.
[8] A. Casnati, A. Pochini, R. Ungaro, C. Bocchi, F. Ugozzoli, R. J. M. Egberink, H. Struijk, R. Lugtenberg, F. de Jong, D. N. Reinhoudt, *Chem. Eur. J.* **1996**, *2*, 436.
[9] S. E. Matthews, P. Schmitt, V. Felix, M. G. B. Drew, P. D. Beer, *J. Am. Chem. Soc.* **2002**, *124*, 1341; S. E. Matthews, N. H. Rees, V. Felix, M. G. B. Drew, P. D. Beer, *Inorg. Chem.* **2003**, *42*, 729.
[10] P. L. H. M. Cobben, R. J. M. Egberink, J. G. Bomer, P. Bergveld, W. Verboom, D. N. Reinhoudt, *J. Am. Chem. Soc.* **1992**, *114*, 10573.
[11] S. E. Matthews, V. Felix, M. G. B. Drew, P. D. Beer, *New J. Chem.* **2001**, *11*, 1355.
[12] P. Schmitt, P. D. Beer, M. G. B. Drew, P. D. Sheen, *Angew. Chem*, **1997**, *36*, 1399; *Angew. Chem. Int. Ed. Engl.* **1997**, *36*, 1840.
[13] S. E. Matthews, V. Felix, M. G. B. Drew, P. D. Beer, *Phys. Chem. Chem. Phys.* **2002**, *4*, 3849.
[14] C. D. Gutsche, M. Iqbal, *Org. Synth.* **1990**, *68*, 234.
[15] C. D. Gutsche, J. A. Levine, *J. Am. Chem. Soc.* **1982**, *104*, 2652.
[16] K. Iwamoto, K. Araki, S. Shinkai, *Tetrahedron* **1991**, *47*, 4325.
[17] Cerius2 v3.5, Molecular Simulations Inc., San Diego (U.S.A.), **1999**.
[18] A. K. Rappe, C. J. Casewit, K. S. Colwell, W. A. Goddard III, W. M. Skiff, *J. Am. Chem. Soc.* **1992**, *114*, 10024.
[19] A. Varnek, G. Wipff, *J. Comput. Chem.* **1996**, *17*, 1520.
[20] W. Kabsch, *J. Appl. Crystallogr.* **1988**, *21*, 916.
[21] SHELX86: G. M. Sheldrick, *Acta. Crystallogr.* Sect. A **1990**, *46*, 467.
[22] G. M. Sheldrick, SHELXL, Program for Crystal Structure Refinement, University of Göttingen, Göttingen (Germany), **1993**.
[23] Z. Otwinowski, W. Minor in *Methods Enzymol.* **1997**, *276*, 307.
[24] A. Altomare, G. Cascarano, G. Giacovazzo, A. Guagliardi, M. C. Burla, G. Ploidori, M. Camalli, *J. Appl. Crystallogr.* **1994**, *27*, 435.
[25] D. J. Watkin, C. K. Prout, J. R. Carruthers, P. W. Betteridge, R. I. Cooper, CRYSTALS issue 11, Chemical Crystallography Laboratory, Oxford (UK), **2001**.

Received: October 21, 2002 [F4518]